International Journal of Research in Engineering and Science (IJRES)
ISSN (Online): 2320-9364, ISSN (Print): 2320-9356
www.ijres.org Volume 10 Issue 6 ǁ 2022 ǁ PP. 1493-1504

Design and Analysis of a Novel High-Gain Dc-Dc Boost Converter with Low Component Count

[1]E. Narasaiah, *PG student, St. Marys group of institutions, Guntur, AP, India*
[2]Lakshmi Narayana, *HOD, St. Marys group of institutions, Guntur, AP, India*

Abstract: *This project proposes a new transformer less quadratic boost converter operated by a single switch for the renewable energy systems. As it is a single switch converter needs single pulse, so the controller is simple and compact. The proposed converter produces high step-up gain with very few components like single active switch, three passive switches and four energy elements. Hence, the size and weight of the converter is low as compared with several high step-up converters. In addition, the proposed boost converter has the advantage of continuous input current, which is suitable for renewable energy applications. The detailed steady state operation is presented in this project with complete theoretical calculations. Comparative discussion is also made in many areas with recently published step-up converters. To test the performance, the proposed quadratic boost converter is simulated in MATLAB/SIMULINK environment.*
Keywords: *DC to DC converter, Quadratic conversation, Boost converter, Single switch*

Date of Submission: 07-06-2022 Date of acceptance: 23-06-2022

I. INTRODUCTION

In recent years, the evolution of power conversion has developed significantly, owing to the long-life batteries that supply energy to embedded systems and many similar gadgets. In response to the need for efficient, compact, and cost-effective high-voltage gain, switch mode DC-DC power converters have flourished over the recent years, to meet the standards of both the domestic and industry sectors. Several new topologies have been proposed in recent years that are intended to cope with this challenge of obtaining high DC voltage gain, while keeping the overall design economical. Nowadays, renewable energy sources are becoming an important subject of research in the field of electrical engineering. It has been estimated that in the near future, the requirement for renewable energy will increase threefold, hence the need for increasingly improved topologies of DC-DC boost converters has become the focus of researchers. In order to meet this need, several universities around the world have introduced undergraduate and graduate level courses on this subject, to disperse the outcomes of related research. In recent years, photovoltaic (PV) panels have achieved commercial success as a reasonable and economical substitute for conventional electricity. Generally, the DC voltage levels provided by PV panels are not high enough to drive domestic lighting. In such lighting equipment, several ultra-bright LEDs are connected in series to obtain high luminescence. These strings of LEDs generally require voltage levels up to 80 V to 100 V, backed by switch-mode boost converters. In such applications, multilevel converters are widely used for their simple structure and higher voltage gain. Another popular scheme that has been adopted to meet the requirements of high-voltage gain in hybrid vehicles and smart homes is a switched-capacitor based converter topology, as presented in. The transportation sector is another noteworthy domain that has gained substantial importance in modern society, both on a social and economic basis. Electric motors that drive modern fully electric vehicles (FEV) are powered by storage batteries or fuel cells that are stacked over each other and produce DC voltage around 100 V, while the DC bus bar in FEVs runs at 400 V DC. Therefore, a high-gain DC boost converter is required to transform the low DC voltage of storage batteries into the high DC voltage for the DC bus bar. The DC-DC boost converter proposed in this paper is a potential solution to such problems, where high-voltage gain is required along with a small physical size of equipment. The proposed converter constitutes one power switch in the form of a power MOSFET, three diodes, two inductors, and two capacitors, hence making the total component count significantly lower than some recently proposed high-voltage gain DC-DC converter designs. The design presented in exploits a cascade topology to achieve high DC voltage gain. The converter in utilizes a quadratic boost converter that is followed by a Cuk converter to achieve significantly higher voltage gain. This approach is adaptable where very high-voltage gain is the prime objective, such as the DC bus bar in fuel-cell vehicles. However, high-voltage gain comes at the cost of considerably larger component count. Although, the converter in uses a single power switch, three inductors, four diodes, and four capacitors make the design implementation larger, hence limiting the scope of applications. In Reference, a new boost converter topology is introduced that allows for a wide input voltage range and achieves high-voltage gain at a moderate duty- cycle. The topology that is proposed in uses two

power switches, six didoes, two inductors, and six capacitors. The voltage gains of the design proposed in is given as $2N$, where N is the number of Dickson bifold multiplier cells integrated with the $(1-D)$ basic interleaved converter. Investigating the topologies proposed in, it can be seen that the high-voltage gain is obtained with a relatively large component count that renders these designs unsuitable for compact areas, such as robotics and embedded systems. The converter presented in this paper proposes a solution to this problem by introducing a new topology, to achieve high voltage gain with a reduced component count, and without significant reductions in efficiency.

II. CONSTRUCTION OF DC-DC CONVERTER

The DC-DC boost converter proposed in this project has one power switch, which is a power MOSFET, three diodes, two inductors, and two capacitors. The topology of this converter is presented in Figure 1. Due to the existence of only one switch, the converter operates in two switching modes: Mode 0 (M0) and Mode 1 (M1). Proposed converter operates in a continuous conduction mode (CCM) and can drive a wide range of resistive loads.

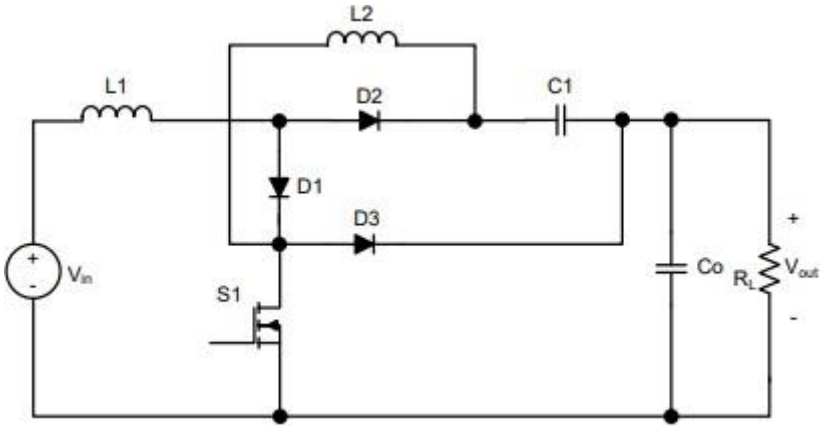

Fig 1: Topology of the proposed DC-DC boost converter

2.1 OPERATION MODES: -

Based on the assumptions, there are two operating modes of the proposed converter. The voltage polarities and current directions are shown in the circuits below. The operating modes are described as follows.

MODE-0(M0): -The MOSFET S1 is turned on, and diode D1 is forward biased and hence starts conducting. This causes the linear flow of current IL1 through the inductor L1, and hence the energy is stored in it. This condition is represented in Figure 2. After passing the short lived transient phase, inductor L2 is also magnetized by the current IL2. The directions of IL1 and IL2 are shown in Figure 2. Power diodes D2 and D3 are off, due to the reverse voltage polarity across them and hence do not conduct. The reason that capacitor C1 is in series with the inductor L2, is that the current IL2 also charges C1 with the voltage polarity as shown in Fig.2. The current that flows through S1 is the algebraic sum of IL1 and IL2.

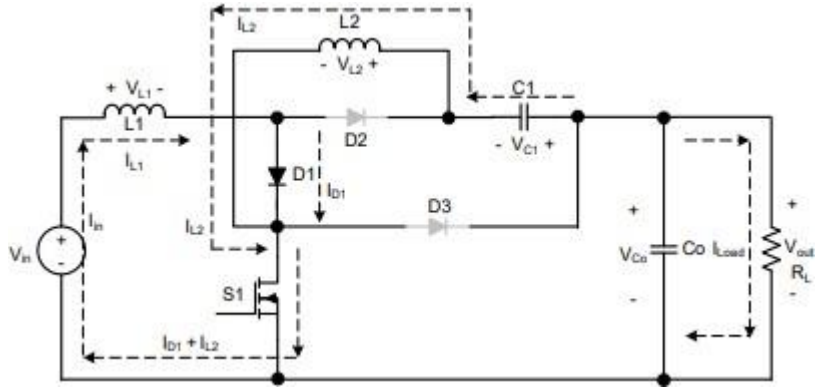

Fig. 2: Voltage polarities and current directions in Mode 0

The voltage across the inductor L1, $V_{L1,ON}$, is only equal to the input DC voltage V_{in},as shown in Figure 2.

$$VL1,ON = Vin \quad (1)$$

The voltage across L2, $V_{L2,ON}$, is the same as the voltage across C1, V_{C1}. Hence,

$$VL2,ON = VC1 \quad (2)$$

MODE-1(M1):- The switch S1 is turned off and the polarity across both L1 and L2 is reversed to maintain the current flow in the same direction as in M0. In this mode, diode D1 is off, due to the reverse bias polarity across it, and diodes D2 and D3 are on, as has been shown in Figure 3.

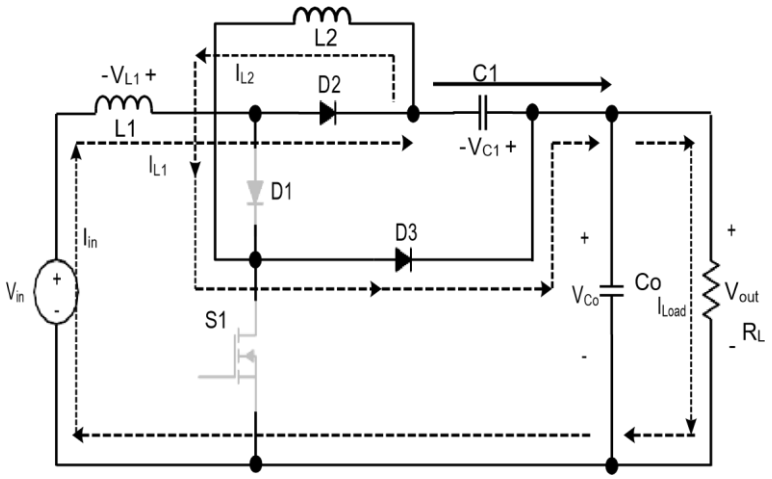

Fig.3: *Voltage polarities and current directions in Mode 1*

The energy that was stored in L1 and L2 is now released and transferred to the capacitors C1 and Co. Capacitor Co starts charging by developing the voltage V_{Co} across it according to the polarity shown in Figure 3. During M1, the voltage $V_{L1,\,OFF}$ across L1 is the difference of the input DC voltage V_{in} and the voltage V_{C1} across C1. Additionally, the voltage $V_{L2,OFF}$ across L2 is the difference between V_{C1} and V_{Co}. These relationships are represented as,

$$VL1,OFF = Vin - VC1 \quad (3)$$

$$VL2,OFF = VC1 - Vout \quad (4)$$

During M0, the time differential dt is equal to the D.T, where D is the duty-cycle and T is the switching period of the S1. Hence,

$$Vin = L1\ diL1/\ D.\ T \quad (5)$$

III. DESIGN OF PROPOSED CONVERTER

Selection of the values of the energy storing component is a critical factor in the behavior and performance of DC-DC converters, no matter which topology is used. The tolerance level in the ripple current of inductors and the ripple voltage of capacitors affects the smoothness and regulation in the output DC voltage levels. As a rule of thumb, the allowable maximum ripple in the inductor current should be no more than 10% of the maximum current that would flow through the inductor. Similarly, the maximum tolerable ripple in the voltage across a capacitor should be no more than 10% of the maximum voltage that will develop across the capacitor. These assumptions set a fair principle for calculating the size of inductors and capacitors for a stable design that produces a smooth level of voltage across the load and provides a constant current. This principle is reflected in the calculations of the inductors and capacitor values used in this proposed boost converter.

Applying volt-second balance on (5) and (6) for L1 gives,

$$\mathbf{Vin \cdot D \cdot T = -(Vin - VC1) \cdot (1 - D) \cdot T}$$

From (2),

$$\mathbf{Vin \cdot D = -Vin + VC1 \cdot (1 - D)}$$

$$\mathbf{VC1 = Vin^{*}(\frac{1}{1-D})}$$

$$\mathbf{G = \frac{Vout}{Vin} = \frac{1}{(1-D)^2}}$$

When S1 is off in M1, the diode D2 becomes on and the S1 becomes parallel to the load. Therefore, the voltage across S1 is the same as Vout.

$$\mathbf{VS1,OFF} = = \frac{\mathbf{V(in1} - \mathbf{D)2}}{\mathbf{Vout}}$$

When D1 is off, the voltage stress across D1, VD1, OFF, can be calculated by applying the KVL around the loop, consisting of D3, Vin, and L1. This gives

$$\mathbf{VD1,OFF} = \mathbf{Vout} \cdot (\mathbf{2D} - \mathbf{D2}) + \mathbf{VL1}$$

The voltage stress across D2 can be calculated by the condition when D2 is off in M0. It can be observed that

$$\mathbf{VD2,OFF} = \mathbf{L2} \cdot \frac{\Delta \mathbf{IL2}}{\mathbf{D} \cdot \mathbf{f_s}}$$

The voltage stress, VD3, OFF, can be calculated by applying the KVL around the loop consisting of D3, S1, and Co during M0. As S1 is on, the voltage across D3 during its off state is the voltage across Co, the Vout. Hence,

$$\mathbf{VD3,OFF} = \frac{\mathbf{Vin}}{(\mathbf{1} - \mathbf{D})^2}$$

4. SIMULATION RESULTS

The simulink model of the a new transformerless single switch quadratic boost converter for renewable energy applications is explained which shows the output waveforms of the converter to justify the statement in the title of high voltage gain and high efficiency and the output waveforms are to be extracted from the MATLAB.

Table.no-1: Circuit parameters for transformer less quadratic boost DC-DC converter

Symbol	Quantity	Value
Vin	Nominal input voltage	25 V
Vo	Output voltage	400 V
Po	Output power	400 W
Fs	Switching Frequency	50 KHZ
L1	Input inductor	375µ H
L2	Second inductor	750µ H
C1	Main Capacitor	12µ F
Co	Output Capacitor	56µ F
M(D)	Gain	16
D	Duty Cycle	75%

The table 1 represents the circuit components which are considered for the MATLAB simulation these are the assumed theoretical values calculated for the transformer less quadratic boost DC-DC converter. The input voltage is taken as 25V with an output voltage expectancy of 400V.The output power is considered as 400W with the load resistance as 400 ohms and switching frequency of 50KHz. Using the voltage conversion ratio M(D) formula the duty cycle is calculated and is given as D=0.75. The inductor current ripples for both the inductors L1 and L2 is taken as 1A, 2A and 0.5A for the capacitors C1 and C0 the voltage ripple is taken as 20V. The inductor values L1, L2 and L_0 and the capacitor values C1, C2 and C_0 are calculated from the formula given in the above table.

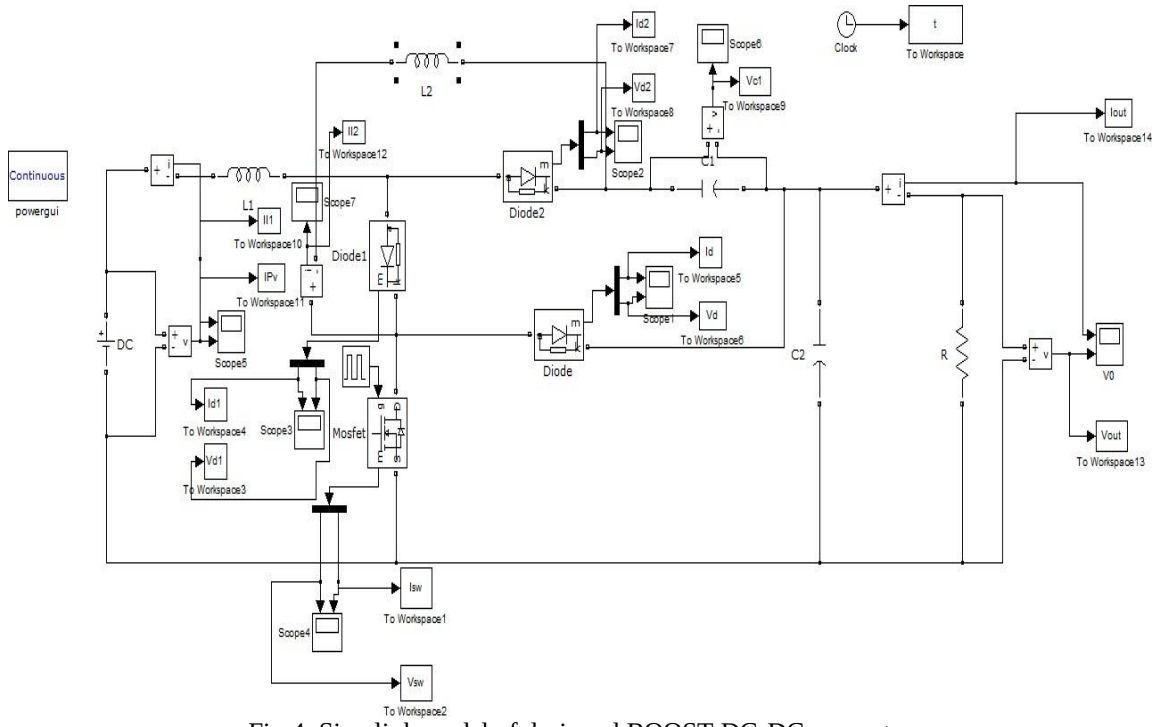

Fig 4: Simulink model of designed BOOST DC-DC converter

The fig. 4 represents the Simulink model of the proposed boost DC-DC converter. The proposed converter consists of single switch, two inductors, three diodes, two capacitors and a load resistance and an input supply source. A single pulse generator is used for the switch as they are synchronously connected to each other. The voltage measurement and the current measurements are connected to all the required components of the Simulink components and the workspace is added to the scopes for obtaining the required graphical waveforms. The IGBT switches are used for efficient output values and the demux multiplier is used for both the switches and both the diodes to obtain both the current and the voltage measurements in a single scope. The powergui is used to obtain the equivalent circuit. The above figure shows the simulation diagram of a proposed Quadratic Boost DC- DC converter here in this Simulink model all the components extracted from the Simulink library and performed the simulation in the MATLAB software.

From the table 2 shows us the performance of the proposed boost DC-DC converter for various duty ratio values of the output voltage, ripple percentage, input power, output power and percentage efficiency. By taking the duty ratio values from 0.1 to 0.8 different output values are obtained. There are a gradual increase of the output voltage values and the ripple factor is less than 1-3%. The respective efficiency values are very high even at the 0.10 duty ratio values and the efficiency values obtained ranges between the values of 89-95% and the highest efficiency value obtained is 93.13%. The output voltage and the ripple factor are obtained from the graphical values obtained from the scope and the efficiency values are calculated using the input and output power values.

Table 2: Performances of the converter of various duty ratios

S.NO	Duty ratio (D)	Output Voltage (Vo)	% Ripple	Pin (W)	Pout (W)	% Efficiency
1	0.10	30.21	0.993	2.4495	2.2814	93.13
2	0.15	33.91	0.884	3.1425	2.8745	91.47
3	0.20	38.32	0.652	4.02	3.671	91.31
4	0.25	43.64	0.137	5.1725	4.7611	92.04
5	0.3	50.14	0.997	6.8825	6.2875	91.35
6	0.35	58.21	0.515	9.44	8.469	89.71
7	0.4	68.36	1.170	13.457	11.682	86.80
8	0.45	81.39	1.165	19.092	16.562	86.74
9	0.5	98.5	1.218	27.7	24.25	87.54

10	0.55	121.5	1.046	41.2	36.9	89.58
11	0.6	153.5	0.781	64.975	58.913	90.67
12	0.65	200.1	1.248	109.75	100.11	91.21
13	0.7	271.6	1.104	198.45	184.38	92.91
14	0.75	387.3	0.361	402.75	375.02	93.11
15	0.8	573.9	1.045	920	823.54	89.51

Table 3: Performance of the proposed converter various duty ratios with voltages of switches and diodes.

Duty Ratio(D)	V(D)	V(D1)	V(D2)	I(D)	I(D1)	I(D2)	V(SW)	I(SW)
0.10	30	3	28	0.16	0.198	0.19	30	0.35
0.15	32	5	29	0.17	0.25	0.25	35	0.44
0.20	39	7	30	0.23	0.3	0.27	39	0.45
0.25	43	11	32	0.26	0.37	0.37	45	0.62
0.30	50	15	35	0.3	0.49	0.52	50	0.71
0.35	59	20	39	0.48	0.7	0.55	59	1.05
0.40	70	28	40	0.58	0.7	0.95	70	1.55
0.45	80	38	45	0.72	1.0	1.4	80	2.1
0.50	99	50	50	0.8	1.7	1.6	100	2.19
0.55	110	70	55	1.23	2.3	1.81	130	3.6
0.60	150	90	60	1.5	2.9	2.9	151	4.6
0.65	200	130	70	2.1	5.4	5.4	200	7.7
0.70	265	190	80	3.2	8.9	8.99	270	12.3
0.75	399	290	95	4.95	16.5	16.6	390	21.5
0.80	550	450	119	8.8	37	37.5	590	46

The table 3 determines the characteristics of switches and diodes with various duty ratios, for different duty ratios the voltages of switches and diodes are characterized, performance of switches and diodes voltages are evaluated from the simulated circuit. The voltage values of both the switches and the diodes are taken from the graphical waveform obtained from the scope and the simulation waveforms are given below in the results section. The simulation results of the QUADRATIC BOOST DC-DC converter are obtained as following

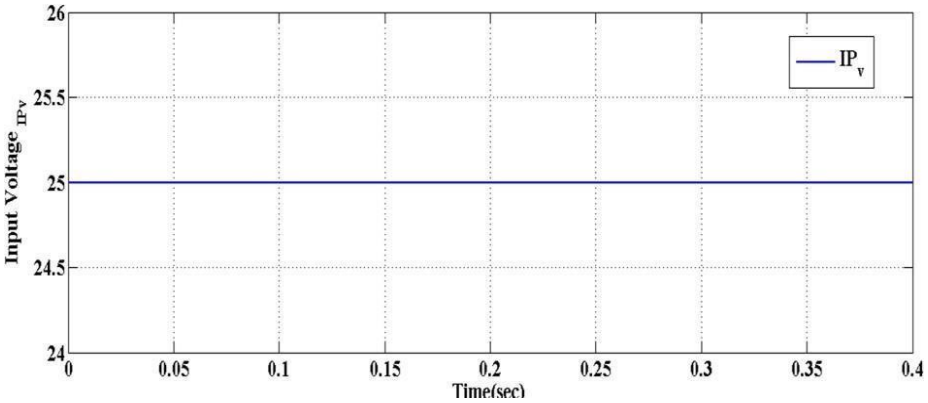

Fig. 5: Simulated waveform of input voltage

The fig. 5 represents the simulated waveform of input voltage for the proposed Boost DC-DC converter with a constant voltage value of 25V. The waveform is obtained between the input voltage and the time axis. The fig 6 gives the simulated waveform of the output voltage for the proposed Boost DC-DC converter and the value obtained is 600V which is nearer to the assumed value. The simulated waveform is considered with time on x-axis and the voltage on y-axis.

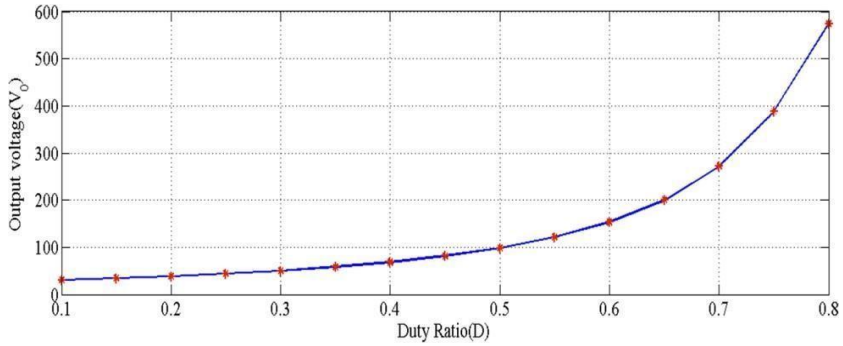

Fig. 6: Simulated waveform of output voltage

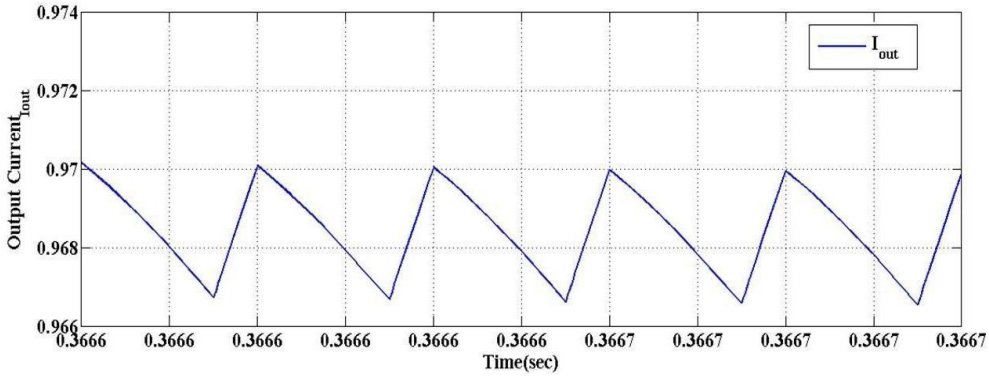

Fig. 7: Simulated waveform of output current

The fig. 7 shows the output current waveform of the proposed boost DC-DC converter which was obtained upon the simulation of the circuit. The waveform has the sawtooth formation and the output current obtained for the D value is given as 0.79A and the simulation is done in the continuous conduction mode. The output current values are required for the tabular values.

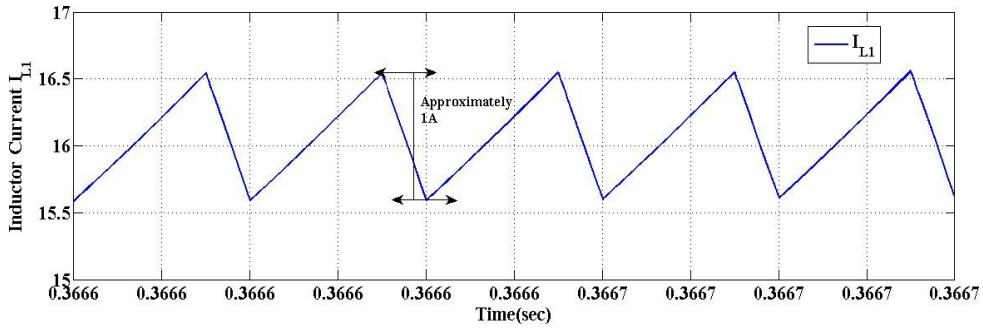

Fig. 8: Simulated waveform of first inductor current

The fig. 8 represents the first inductor current value which is obtained upon the simulation of the proposed boost DC-DC converter and the current ripple factor for the inductor L_1 is taken as 1A. The average current value obtained for the I_{L1} is observed.

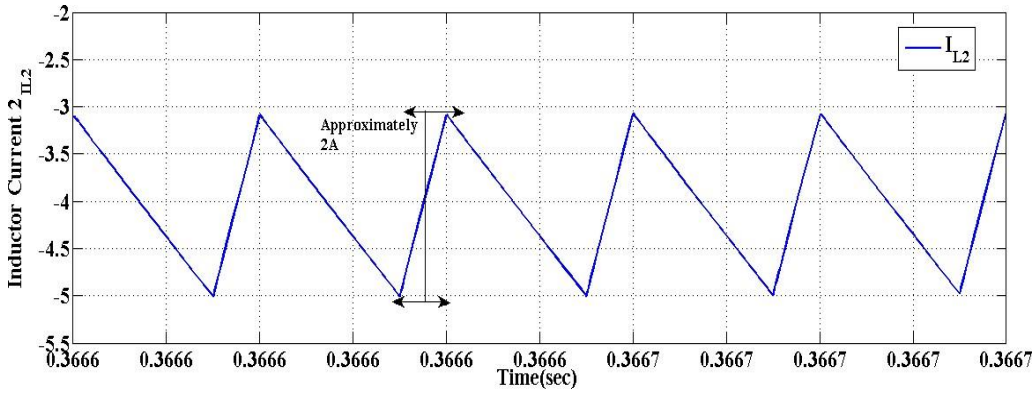

Fig. 9: Simulated waveform of second inductor current

The fig. 9 represents the second inductor current value which is obtained upon the simulation of the proposed boost DC-DC converter and the current ripple factor for the inductor L_2 is taken as 2A. The average current value obtained for the I_{L2} is observed. For both the inductor the average current values are considered.

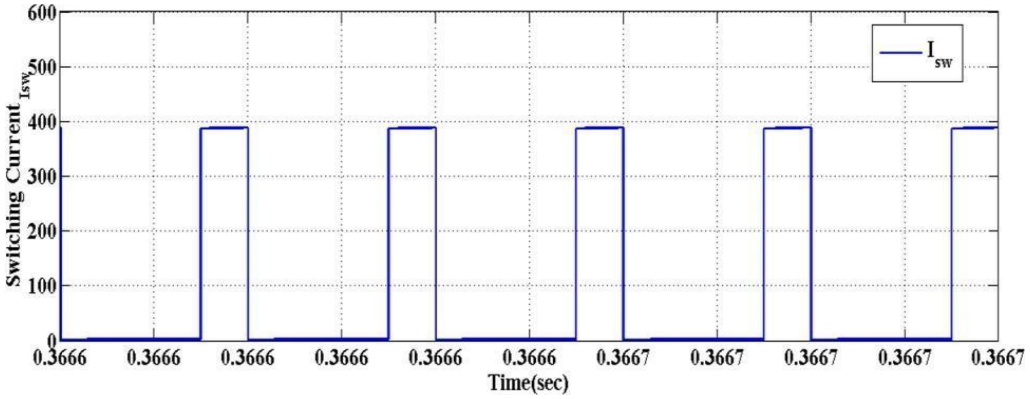

Fig. 10: Simulated waveform of switch current.

The fig. 10 represents the simulated waveform of current of the one of switch S1 which is obtained upon the simulation of the proposed boost DC-DC converter and the current values of the switch is given as 21.5A. The y-axis is considered as first switch current and the x-axis is taken as the time proportion of 0.3666sec to 0.3667sec.

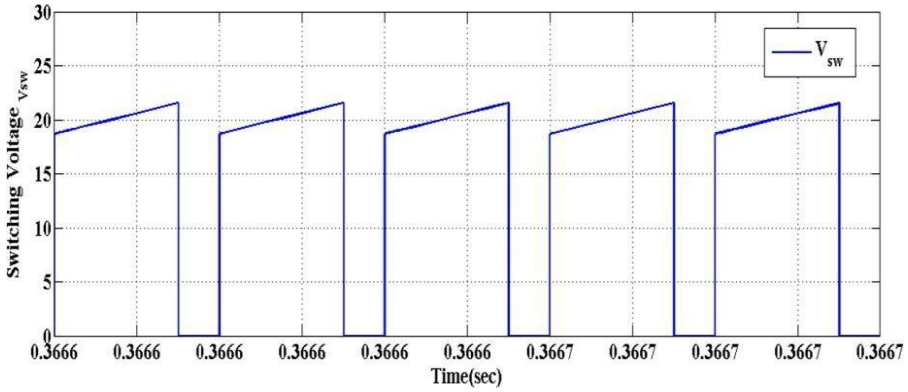

Fig. 11: Simulated waveform of switch voltage

The figure 11 illustrates the simulated waveform first switch voltage which is 23.5 volts obtained upon the simulation of proposed boost DC-DC converter. The simulated waveform is of the rectangular type waveform. The time axis is represented on x-axis which has a each division value of 0.3666 seconds. The voltage (V) is plotted on y-axis with an interval of 5 volts.

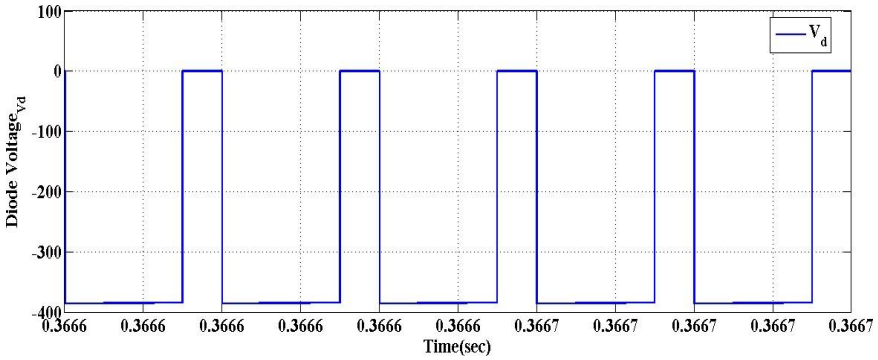

Fig. 12: Simulated waveform of first diode voltage.

The figure 12 illustrates the simulated waveform first diode voltage which is 400 volts obtained upon the simulation of proposed boost DC-DC converter. The simulated waveform is of the rectangular type waveform. The time axis is represented on x-axis which has each division value of 0.3666 seconds. The voltage (V) is plotted on y-axis with an interval of 100 volts.

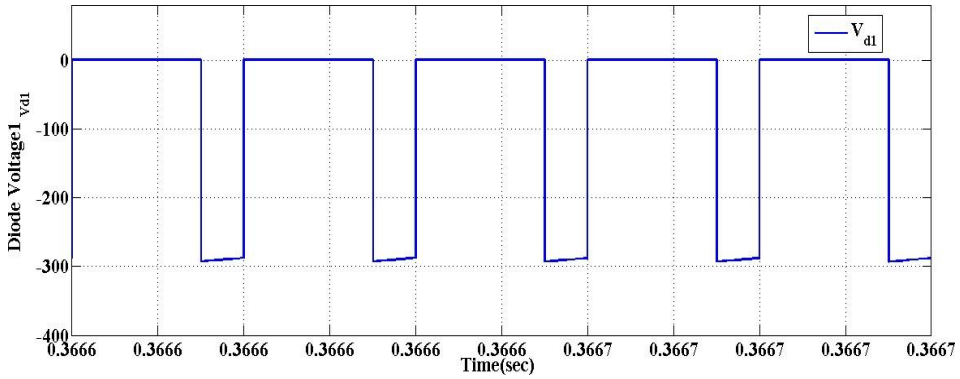

Fig. 13: Simulated waveform of second diode voltage.

The figure 13 illustrates the simulated waveform second diode voltage which is 300 volts obtained upon the simulation of proposed boost DC-DC converter. The simulated waveform is of the rectangular type of waveform. The time axis is represented on x-axis which has an each division value of 0.3666 seconds. The voltage (V) is plotted on y-axis with an interval of 100 volts.

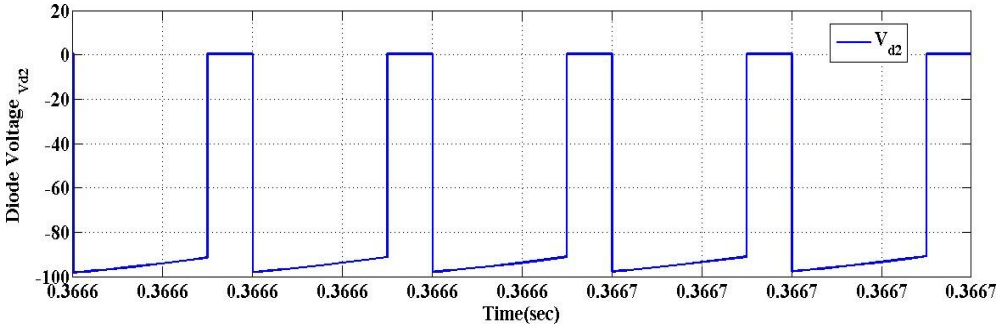

Fig. 14: Simulated waveform of third diode voltage.

The figure 14 illustrates the simulated waveform third diode voltage which is 100 volts obtained upon the simulation of proposed boost DC-DC converter. The simulated waveform is of the rectangular type of waveform. The time axis is represented on x-axis which has each division value of 0.3666 seconds. The voltage (V) is plotted on y-axis with an interval of 20 volts.

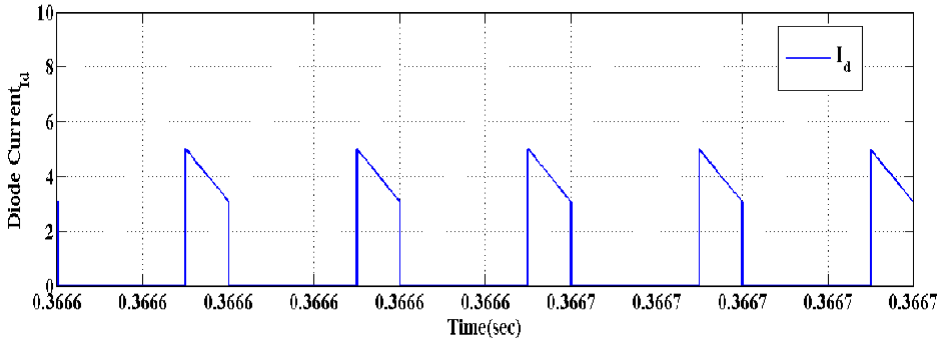

Fig. 15: Simulated waveform of first diode current.

The figure 15 illustrates the simulated waveform first diode current which is 3 A obtained upon the simulation of proposed boost DC-DC converter. The simulated waveform is of the rectangular type of waveform. The time axis is represented on x- axis which has each division value of 0.3666 seconds. The current (A) is plotted on y-axis with an interval of 2 ampere.

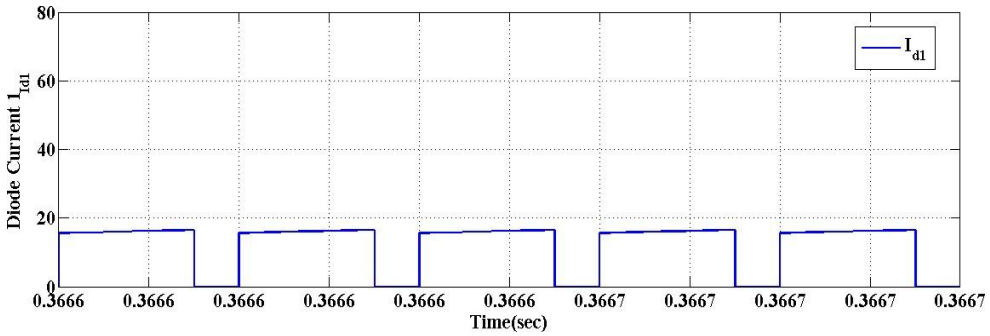

Fig. 16: Simulated waveform of second diode current.

The figure 16 illustrates the simulated waveform second diode current which is 15A obtained upon the simulation of proposed boost DC-DC converter. The simulated waveform is of the rectangular type of waveform. The time axis is represented on x-axis which has each division value of 0.3666 seconds. The current (A) is plotted on y-axis with an interval of 20A.

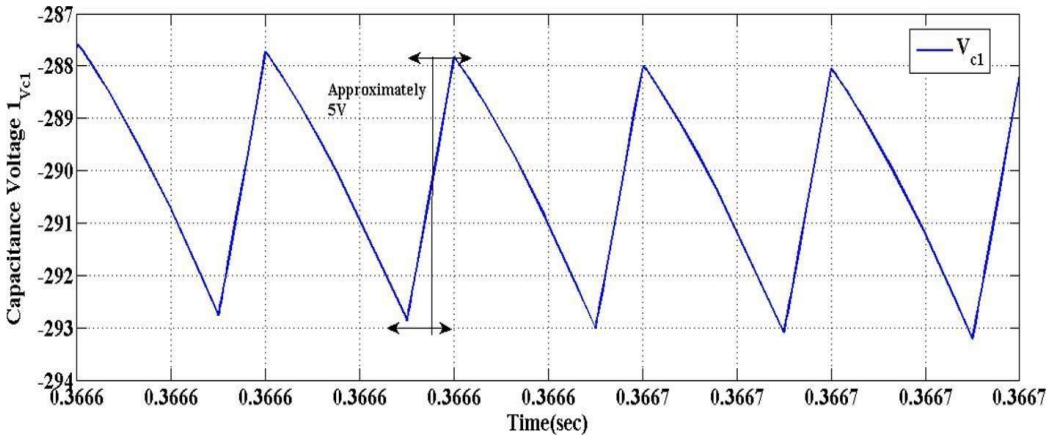

Fig. 17: Simulated waveform of capacitor voltage.

The figure 17 illustrates the simulated waveform pump capacitor voltage which is 288.5volts obtained upon the simulation of proposed boost DC-DC converter. The simulated waveform is of the sawtooth type of waveform. The time axis is represented on x-axis which has each division value of 0.3666 seconds. The voltage (V) is plotted on y-axis with an interval of 24 volts. The ripple voltage of the capacitor is taken as 1V.

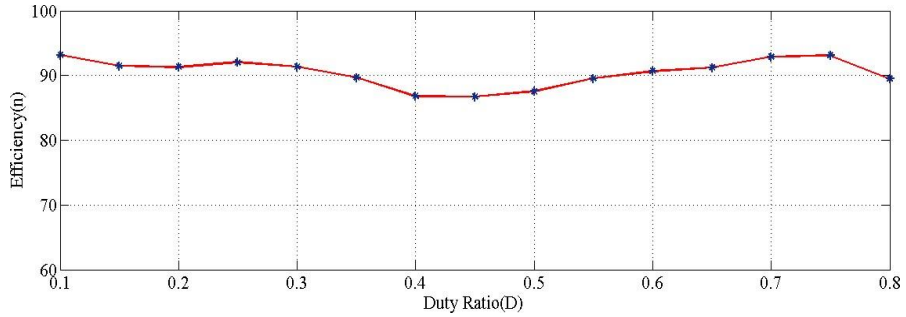

Fig. 18: The efficiency graph for various duty ratios.

From table 2 shows the various duty ratios ranging from 0.1 to 0.8 the efficiency values which are obtained are plotted in fig 18. The duty ratio values are taken on the x-axis from 0.1 to 0.8 and the efficiency percentage is taken on y-axis with an interval of 10%. There are a gradual increase of the efficiency percentage values.

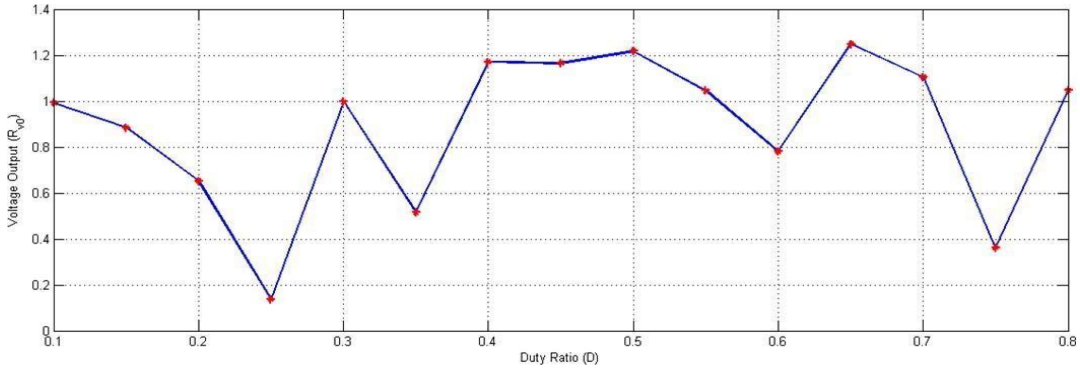

Fig-4.17: The ripple factor for various duty ratios.

From table 4.17 for the various duty ratios ranging from 0.1 to 0.8 the ripple factor values which are obtained are plotted in fig 4.17. The duty ratio values are taken on the x-axis from 0.1 to 0.8 and the ripple factor is taken on y-axis with an interval of 0.2. The ripple factor values are low and does not exceed beyond the value of 1.4.

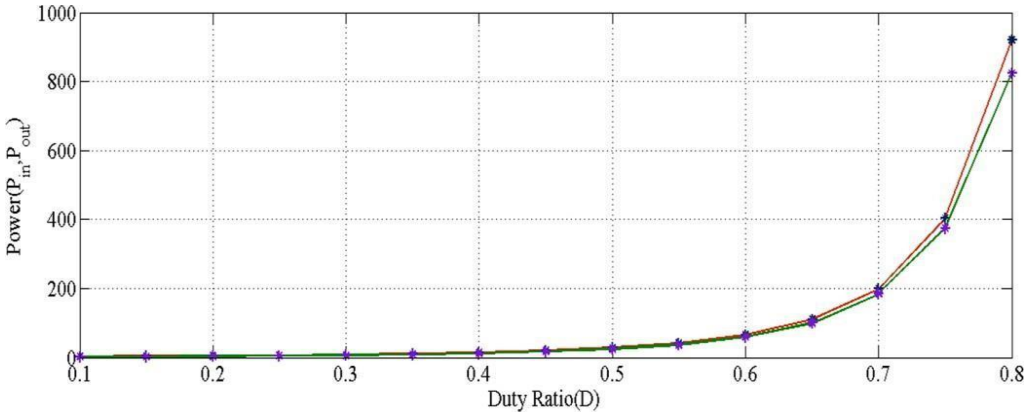

Fig-4.18: The graph shows input and output power values for various duty ratios.

From table 4.19 for the various duty ratios ranging from 0.1 to 0.8 the input and output power values which are obtained are plotted in fig4.19. The duty ratio values are taken on the x-axis from 0.1 to 0.8 and the output voltage is taken on y-axis with an interval of 200 Watts. The input and output values of the proposed boost DC-DC converter are calculated and placed in table 4.19 and both the power values are compared and plotted which gives the accurate values resulting in the efficient outcome results of the converter.

IV. CONCLUSION

In this paper a new DC-DC boost converter is presented that utilizes a low component count in comparison to some recently proposed high DC voltage gain boost converters. The proposed boost converter was simulated for the DC voltage gain, voltage stresses, and efficiency. The simulation results proved the validity of the proposed design. A 250 Watts prototype model was designed and simulated, and the results were compared with very recently published designs of boost converters, based on component count and component sizing. The comparison clearly revealed that the proposed design promisingly met the objective of achieving high-voltage gain, while keeping the component count low.

REFERENCES

[1]. Shahir, F.M.; Babaei, E. Extended topology for a Boost DC-DC Converter. IEEE Trans. Power Electron. 2019, 34, 2375– 2384.
[2]. Bhaskar, M.S.; Almakhles, D.J.; Padmanaban, S.; Blaabjerg, F.; Subramaniam, U.; Ionel, D.M. Analysis and Investigation of Hybrid DC–DC Non-Isolated and Non-Inverting Nx Interleaved Multilevel Boost Converter (Nx-IMBC) for High Voltage Step-Up. Applications: Hardware Implementation. IEEE Access 2020, 8, 87309–87328.
[3]. Ferdowsi, A.M.; Shamsi, P. A Family of Scalable Non-Isolated Interleaved DC-DC Boost Converters with Voltage Multiplier Cells. IEEE Access 2019, 7, 11707–11721.
[4]. Jiang, W.; Chincholkar, S.H.; Chan, C.-Y. Investigation of a Voltage-Mode Controller for a dc-dc Multilevel. Boost Converter. IEEE Trans s. Circuits Syst. II Express Briefs 2018, 65, 908–912.
[5]. Nguyen, M.-K.; Duong, T.-D.; Lim, Y.C. Switched-Capacitor-Based Dual-Switch High-Boost DC–DC Converter. IEEE Trans. Power Electron. 2018, 33, 4181–4189.
[6]. Khaligh, A.; Li, Z. Battery, Ultra-capacitor, Fuel Cell, and Hybrid Energy Storage Systems for Electric, Hybrid Electric, Fuel Cell
[7]. Lai, C.-M.; Cheng, Y.-H.; Hsieh, M.-H.; Lin, Y.-C. Development of a BidirectionalDC/DC Converter with Dual-Battery EnergyStorage for Hybrid Electric Vehicle System. IEEE Trans. Veh. Technol. 2017, 67, 1036–1052.
[8]. Forouzesh, M.; Siwakoti, Y.P.; Gorji, S.A.; Blaabjerg, F.; Lehman, B. Step-Up DC–DC Converters: A Comprehensive Review of Voltage-Boosting Techniques, Topologies, and Applications. IEEE Trans. Power Electron. 2017, 32, 9143–9178.
[9]. Pires, V.F.; Cordeiro, A.; Foito, D.; Silva, J.F. High Step-Up DC-DC Converter for Fuel Cell Vehicles Based on Merged Quadratic Boost-Cuk. IEEE Trans. Veh. Technol. 2019, 68, 7521–7530.
[10]. Zhang, Y.; Liu, H.; Li, J.; Sumner, M.; Xia, C. DC–DC Boost Converter with a Wide Input Range and High Voltage Gain for Fuel Cell Vehicles. IEEE Trans. Power Electron. 2018, 34, 4100–4111.
[11]. Ferdowsi, A.A.M.; Shamsi, P. High-Voltage-Gain DC-DC Step-Up Converter with Bifold Dickson Voltage Multiplier Cells. IEEE Trans. Power Electron. 2019, 34, 9732–9742.